Excited Triplet States in Aggregates and Monomers of Water Soluble Meso-Aryl Substituted Porphyrins

Héctor García-Ortega,[†,§] José L. Bourdelande,*[,‡] Joaquim Crusats,[†] Zoubir El-Hachemi,[†] and Josep M. Ribó*[,†]

Department of Organic Chemistry, University of Barcelona, c. Martí i Franquès 1, 08028-Barcelona, Catalonia, Spain and Department of Chemistry, Autonomous University of Barcelona, 08913-Bellaterra, Catalonia, Spain

Received: November 25, 2003; In Final Form: February 10, 2004

The excited triplet states of a set of water-soluble 4-sulfonatophenyl meso-bis and meso-tetrakis substituted porphyrinoids were studied in a wide range of concentrations. All of these porphyrinoids show the formation of π-stacked aggregates (H aggregates). As a consequence of the 5,15-diaryl substitution, and of aggregation, two excited triplet states can be detected, the more stable being accessible only by internal conversion of the current excited-state T_1. The aggregates showed a significant singlet oxygen quantum yield [$^1O_2$ ($^1\Delta_g$), determined by the phosphorescence method], which in most cases was of the same order as the monomeric forms.

Introduction

The photophysical properties of condensed phases of porphyrinoids are of high chemical and biological significance. Porphyrinoids and metalloporphyrinoids are well-known as triplet state photosensitizers (see, e.g., ref 1−7), and this property is already being used in photodynamic tumor therapy, where the action mechanism is mostly attributed to the photosensitization of dioxygen [$^3O_2$ ($^3\Sigma_g^-$) → $^1O_2$ ($^1\Delta_g$)].[8] The dependence of the photophysical properties of porphyrinoid supramolecular systems on the spatial ordering of the porphyrinoid building blocks is used by living organisms to obtain different biological functions from similar chromophores.[9] If electron-transfer or energy-transfer processes follow the initial light absorption, it will depend on the geometry of such arrangements.[10] That porphyrins easily aggregate is well established.[11] However, only in the past few years has the aggregation of water soluble porphyrins been studied systematically (see, e.g., ref 12−15), and a self-evident general conclusion is that the extensive planar π system of these compounds originates strong hydrophobic effects. Additional electrostatic interactions and hydrogen bonds lead to defined geometries.

Aggregation is often seen as a disadvantage for photosensitizing applications: e.g., the photophysical properties of inclusion complexes of water-soluble meso-tetrasubstituted porphyrins with cyclodextrins has been studied in order to obtain nonaggregated porphyrins in aqueous solutions.[16] It is worth noting here that one of the objectives of photodynamic therapy is the selective concentration of the photosensitizer in tumor cells. Furthermore, photosensitizer uptake occurs preferentially in defined sites,[17] or defined organelles, of the cell. This is explained in terms of the different chemical affinities of the cell membranes, to the water structure around the biopolymers and macromolecular crowding[18] in these organelles. Furthermore, understanding how aggregation affects the photophysical behavior of chromophores is not only important for their behavior in biological systems but also for the use of their condensed phases in advanced materials, for example in organic photoconductors or nonlinear optical devices (see, e.g., refs 19 and 20).

Here we report the effects of aggregation in water soluble porphyrins (Figure 1), their excited triplet states, and their capabilities to generate $^1O_2$ ($^1\Delta_g$) by photosensitation.

Experimental Section

Mg Chlorophyllin (MgChl: Soquiber-Lab Cosp, SA, Berga, Spain), Zn tetrasulfonatophthalocyanine, and Cu tetrasulfonatophthalocyanine ($ZnPcS_4$, $CuPcS_4$ Aldrich) were of commercial origin and used without purification. 5,15-Bis(4-sulfonatophenyl)porphyrin-2-sulfonic acid presidium salt (DIPS), 10-bromo-5,15-bis(4-sulfonatophenyl)porphyrin-2-sulfonic acid trisodium salt ($BrDPPS_3$), and 5,10,15,20-Tetrakis(4-sulfonatophenyl)-porphyrin tetrasodium salt ($TPPS_4$) were synthesized, purified, and identified as previously described.[13,21] The corresponding metallo-derivatives $ZnDPPS_3$, $ZnBrDPPS_3$, and $ZnTPPS_4$ were obtained, purified, and identified by the metal oxide method:[22] purification by ion exchange through Amberlite 140 converted the substances to their sodium sulfonate forms.

UV/vis spectra were recorded with a Cary-Varian 5E spectrophotometer: cuvettes ranging in thickness from 1 to 0.01 cm were used for measuring the absorption spectra. Fluorescence spectra were recorded using a SLM-Aminco Bowman instrument; 1 cm light path cuvettes were used for all experiments with exception of some highly concentrated solutions, for which a triangular cuvette was used. ^1H NMR spectra were recorded using a Brucker DMX-500 (500 MHz) in D_2O and using TMS as external reference in the aggregation studies. For the attribution of signals NOE pulse sequences were also used.

Laser flash photolysis studies were performed using as an

* To whom correspondence should be addressed. (J.M.R.) Tel: 34-934021251. E-mail: jmr@qo.ub.es. (J.L.B.) Tel: 34-935811983. Fax: 34-935811265. E-mail: joseluis.bourdelande@uab.es.

† University of Barcelona.

‡ Autonomous University of Barcelona.

§ This work is part of the Ph. D. Thesis of H.G.-O. Present address: Department of Organic Chemistry, Chemistry Faculty, National Autonomous University of Mexico, Ciudad Universitaria 04510, Mexico, D.F.

10.1021/jp037587z CCC: $27.50
Published on Web 03/19/2004

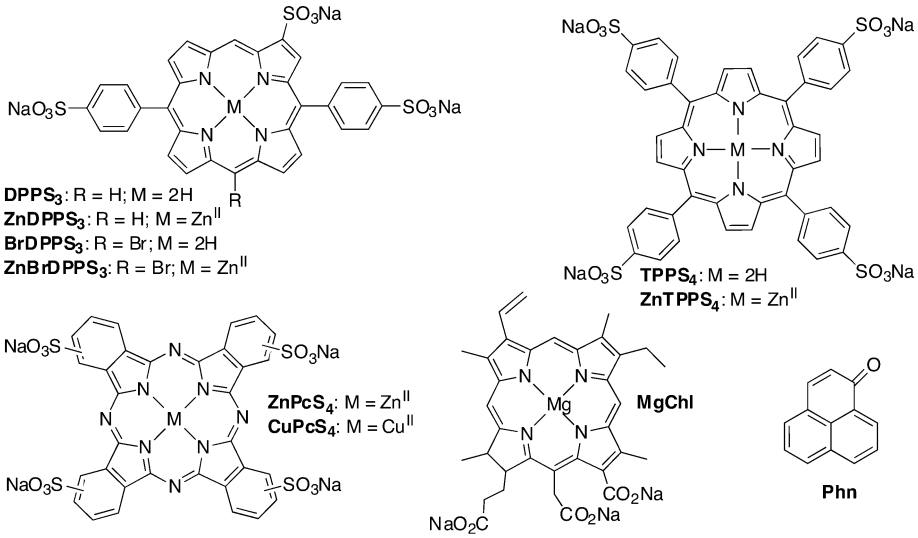

Figure 1. Constitutional formula and abbreviations of the tested compounds.

excitation source a Nd:YAG laser (355 nm: pulse duration 9 ns; Spectron Laser Systems SL404G, maximum potency 155 mJ at 532 nm), which was directly used (phthalocyanines) or modified to 420 nm (porphyrins) by an OPO−S-355 (GWU). The absorption study was made using a Xe lamp (150 W) compressed by an arc pulser (Applied Photophysics) and monochromator (05−109 Applied Photophysics). The recordings were recovered in an oscilloscope Agilent Infiniium 500 MHz, transferred to an Accorn PCRisk station and the analysis was performed using the software LASER and GLint of Applied Photophysics. Decay kinetics were measured at fixed wavelength with a series of individual laser shots, which were averaged and analyzed by computerized nonlinear least-squares iteration. The reported relative yields of excited triplet states correspond to a laser intensity relative to the saturation of the transitory absorption spectra (2.2 mJ/pulse series of 16−64 pulses, depending on the experiment). The differential absorption spectra were obtained from the decays at different wavelengths ($\Delta\lambda = 10$ nm) at several time points after the excitation. A minimum of 20 kinetic traces at different wavelengths were analyzed by single and global analysis methodology with the software cited above (experimental detection limit ≥ 50 ns). No significant differences were detected between the two methods. The spectra were recorded in D_2O solutions at several concentrations between 1×10^{-7} M and 1×10^{-3} M, and in 1 cm thickness cuvettes. Experiments were carried out in pure N_2 atmosphere and in air and pure O_2 saturated solutions, i.e., at 20 °C 0.24 mM and 1.7 mM respectively.[23] Samples of high concentrations showing self-absorbing phenomena were discarded.

For the $^1O_2$ studies, the solutions, concentrations, and excitation modes were the same as for the excited triplet state absorption measurements. Singlet molecular oxygen [$^1O_2$ ($^1\Delta_g$)] was detected by its phosphorescence (S) at 1270 nm using a Ge photodiode (EI−P Edinburgh) equipped with filters Spectrogon (LP-1000 and BP-1275-080-B) and cooled with liquid N_2. Emission and absorption yields were measured by computer extrapolation of the first order decay profile to the center of the laser pulse. Yields of singlet oxygen were obtained, as previously described:[24] measuring the emission intensity as a function of the laser intensity for the sample and for a reference with known Φ_Δ; the initial singlet oxygen emission [$S(t = 0)$] was inferred from the decay extrapolation to time zero and the relationship between this initial intensity and the excitation photon density was determined in the laser energy (E_l) range of 1−3 mJ (linear for all results reported here). The slopes $S(t = 0)/E_l$ [see eq 1] of these linear relationships at several concentrations were measured. The relative quantum yield was calculated from the linear relationship between these slopes in respect to ($1-10^{Abs}$): the $^1O_2$ quantum yield value was inferred from the ratio of this last slope with respect to that of the reference substance [eq 2: perinaphthenone (Phn: Figure 1), $\Phi = 0.95$][25,26]

$$S(t=0) = (k/n^2)k_r\Phi_\Delta(E_l(1 - 10^{-Abs})/LhV\nu) \qquad (1)$$

where k is a proportionality constant, n is the refractive index, k_r is the radiative deactivation constant, Abs is the absorbance at the laser excitation wavelength, V is the irradiated volume, and ν is the frequency of the laser

$$\Phi_{\Delta,\text{sample}} = \Phi_{\Delta,\text{reference}}\{[\partial S(t=0)/\partial E_l]_{\text{sample}}/[\partial S(t=0)/\partial E_l]_{\text{reference}}\} \qquad (2)$$

Results and Discussion

First, we present results on the aggregation in water of the porphyrinoids represented in Figure 1. This was studied by UV/vis and fluorescence spectroscopy (Lambert−Beer law deviations, fluorescence quantum yield variations, and changes in the wavelength of the absorption or emission maxima) in the concentration ranges $1 \times 10^{-6}-1 \times 10^{-3}$ M and $1 \times 10^{-7}-1 \times 10^{-4}$ mol L^{-1}, respectively. In some cases, ^1H NMR experiments at variable temperature and different concentrations were also performed. To infer whether the time-resolved studies on transient species should be attributed to the aggregate or to the monomeric species, we discuss the basic trends of the structure of these aggregates inferred by the simple model of the exciton coupling between chromophores.

Second, we describe the detection of excited states, for different degrees of aggregation (1×10^{-7} M−1×10^{-3} M), through the absorption decays after pulsed laser excitation at the $S_0 \rightarrow S_2$ transition (B- or Soret-band). This was performed both anaerobically and in the presence of O_2. Finally, we show the ability of these compounds to photosensitize O_2, at several degrees of aggregation and in experimental conditions similar to those of the excited-state studies.

Stationary Spectroscopy. All tested porphyrinoids show by UV/vis spectroscopy deviations from the Lambert−Beer law (hypochromic effects) but at very different threshold concentra-

TABLE 1: Electronic Spectra of Aggregated and Monomeric Porphyrinoids[a]

	UV/vis absorption spectra[b]			fluorescence spectra (λ_{exc} = B-band)		
	Lambert−Beer law threshold value (mol L^{-1})	λ_{max} (nm) monomer	λ_{max} (nm) aggregate	threshold value for the decrease of Φ_{emis} (mol L^{-1})	λ_{emis} (nm) monomer	λ_{emis} (nm) aggregate
$DPPS_3$	3.6×10^{-5}	407, 509, 543, 573, 625	394, 512, 547, 576, 633	4×10^{-6}	632, 694	632, 694
$ZnDPPS_3$	[c]4.0×10^{-4}	415, 548, 587	415, 548, 587	4×10^{-6}	595, 650	595, 650
$BrDPPS_3$	3.0×10^{-5}	415, 517, 552, 585, 640	400, 521, 558, 593, 649	5×10^{-7}	646, 705	646, 705
$ZnBrDPPS_3$	4.0×10^{-4}	424, 559, 599	423, 560, 600	4×10^{-6}	609, 655	609, 655
$TPPS_4$	1.0×10^{-4}	412, 516, 553, 580, 636	413, 516, 553, 580, 636	3×10^{-6}	645, 704	645, 704
$ZnTPPS_4$	1.6×10^{-4}	421, 553, 595	421, 556, 596	4×10^{-6}	608, 659	608, 659
MgChl	1.9×10^{-4}	405, 643	401, 504, 655	3×10^{-5}	661, 716	661, 716
$ZnPcS_4$	1.8×10^{-4}	635, 676	637, 682	6×10^{-6}	682	682

[a] For more details see the Supporting Information and Figure 1. [b] B- and Q-bands for porphyrins and chlorophyllin, and Q-bands for phthalocyanines. [c] Solubility limit.

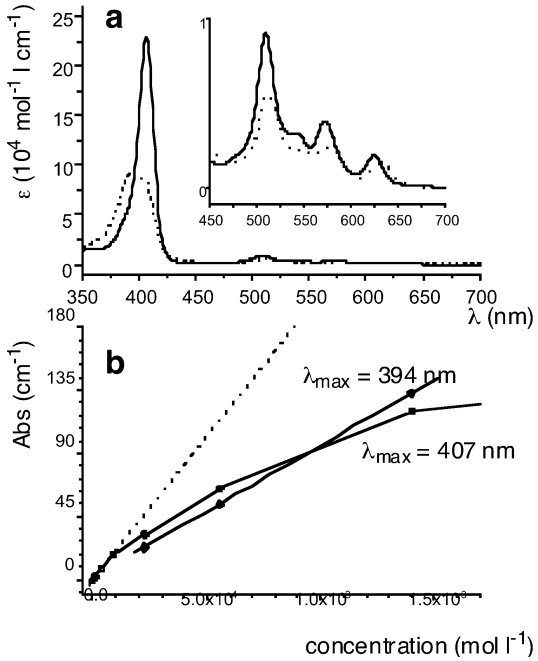

Figure 2. UV/vis absorption spectra of $DPPS_3$: (a) (—) 2.9 10^{-6} M and (···) 1.4 10^{-3} M; (b) variation with the concentration of the B-band absorbances of monomer (λ_{max} 407 nm: −•−) and aggregate (λ_{max} 394 nm: −◆−).

tion values (see Table 1, the example in Figure 2 and the Supporting Information). For example, depending on their absorption spectra, $DPPS_3$ and $BrDPPS_3$ aggregate at concentration values 1 order of magnitude lower than the rest of the compounds. $DPPS_3$, $BrDPPS_3$, and MgChl at high concentrations show blue-shifted B-bands: $DPPS_3$ and $BrDPPS_3$ of $\Delta E \approx 850$ cm^{-1} and MgChl of $\Delta E \approx 250$ cm^{-1}). The remainder of the tested compounds, despite showing hypochromic effects with concentration, did not show bathochromic or hypsochromic shifts in the wavelength maxima of their B-bands.

The fluorescence experiments show that the emission quantum yield begins to decrease, due to concentration effects at threshold values 1 or 2 orders of magnitude lower than those detected due to hypochromic effects of their absorption spectra (Table 1). It is worth noting that the lifetime of the excited singlet state S_1 of these compounds is in the ns and ps range,[27,28] i.e., several orders of magnitude shorter as compared to the accepted collision frequency[29] ($Z_{AA^*} \leq 2.5 \times 10^{10}$ mol^{-1} L s^{-1}) at concentration values where the emission quantum yield decrease is detected. As a consequence, this decrease of the fluorescence intensity should be attributed to the formation of new species and not to the deactivation by collision between a single state excited molecule and an unexcited one. Moreover,

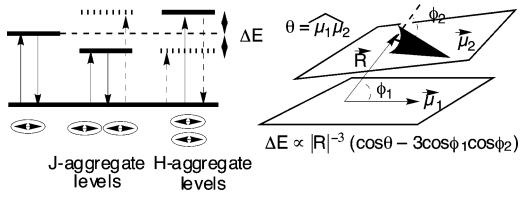

Figure 3. Scheme of the point-dipole approximation of the exciton coupling model (refs 30−32) for a 3D system of two chromophores (angle between transition dipole moments = θ). The side-to-side ordering (J aggregation; $\theta = 0°-90°$: $\phi_1 = \phi_2 = 0°$) or the face-to-face aggregation (H aggregation; $\theta = 0°-90°$: $\phi_1 = \phi_2 = 90°$) show different radiative excitation and deactivation ways (forbidden - - -, allowed —).

when aggregation occurs, the fluorescence spectra did not show changes (wavelength emission maxima and relative intensities of the characteristic double shaped emission band of porphyrins) compared to the corresponding monomeric species; that is, only the quantum yield decrease of the monomer fluorescence could be detected. All of this points to aggregates without any significant fluorescence emission.

The point−dipole approximation of the exciton coupling between chromophores gives a qualitative explanation of the electronic spectra differences between monomer and aggregates.[30−32] In the case of porphyrin aggregates or porphyrin supramolecular systems, this simple model allows the differentiation among side-to-side (J aggregates), face-to-face (H aggregates) and other types of arrangements (see, e.g., refs 33−36). The differentiation criteria for H and J aggregates is a hypsochromic or a bathochromic shift respectively of the chromophore absorption (Figure 3). It is worth noting here that the application of the point-dipole model in porphyrins is usually performed on the $S_0 \rightarrow S_2$ transition (B- or Soret-band), principally because the high exciton-coupling shift originates from the great oscillator strength of the B-band but also because it is not significantly affected by the vibrational changes originating from the homo-association. In contrast, the Q-bands show an important vibrational progression; that is, they are affected by conformational changes in the porphyrin units, and as a consequence, the differences between the $S_0 \rightarrow S_1$ bands of monomer and aggregate are both due to the exciton coupling perturbation and to the conformational changes. The exciton coupling model also predicts low quantum fluorescence yields in the case of H aggregation.[30] The transition from the high to the low excitonic perturbed state is forbidden, and as a consequence, the intersystem crossing toward the excited triple state is favored. In this respect, the aggregates of $DPPS_3$, $BrDPPS_3$, and MgChl show absorption spectra with bathochro-

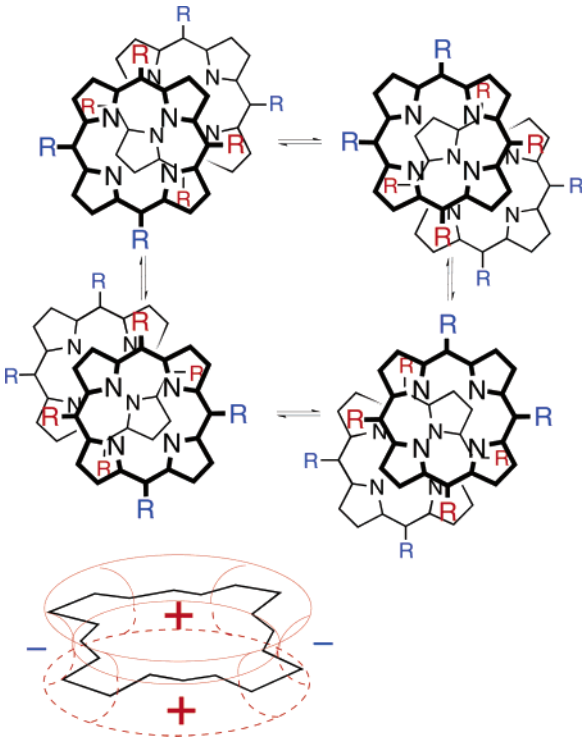

Figure 4. Four degenerate structures of a π-stacked porphyrin dimer (approximate geometry according to refs 37 and 38). In the case of aggregation, the rapid exchange and the aromatic ring current results in high field shifts for the β-pyrrolic protons and those of the meso substituents near to the porphyrin ring (e.g., ortho-phenyl positions in the case of $TPPS_4$).

mic shifted B-band and no significant fluorescence emission, which points to H aggregates, i.e., face-to-face π-stacked aggregates.

The remaining tested porphyrinoids did not show significant shifts of their absorption bands, but their emission yields decreased in a similar way to those of porphyrins showing a bathochromic shift of their B-band. Furthermore, despite the absence of hypsochromic shifts for these compounds, the ^{1}H NMR spectra at several concentrations and at different temperatures point to the formation of the π-staked aggregates. This is the case with $TPPS_4$, which, at a concentration of about 1×10^{-3} mol L^{-1}, its UV/vis spectrum does not show any significant B-band shift (hypochromic effect $\approx$ 15%), although its ^{1}H NMR spectrum (D_2O) indicates a significant concentration ($\approx$20%) of π-stacked aggregate: the protons at the 2′,6′ (meso-phenylic) and β-pyrrolic positions show, with concentration, significant chemical shifts toward high fields (see the Supporting Information). Taking into account the high magnetic anisotropy of the porphyrin ring due to its aromatic current,[37] this implies an aggregate with π-stacked structure (see Figure 4). Furthermore, at high aggregation levels, it is possible to differentiate between the β-pyrrole H atoms of monomer and aggregate, which allows an approximate quantitative analysis of the homoassociation of $TPPS_4$ (see the Supporting Information). For very dilute solutions, the results show an approximate adjustment to a trimer stoichiometry, i.e., a not very high tendency to associate compared to other water soluble porphyrinoids (e.g., $DPPS_3$).

The geometry for a π-stacked dimer of a porphyrin corresponds to a geometry determined principally by the $\pi-\sigma$ interactions.[38] In this respect, Figure 4 shows the commonly accepted dimer structure. With equal substituents at the four meso positions (tetrakis substitution) and unsubstituted β-pyrrolic positions, it results in four degenerate structures: the fast exchange results in average ^{1}H NMR signals and in high field shifts for the protons at the ortho positions of the meso-phenyl substituents and at the β-pyrrolic positions. However, this apparently does not agree with the absence of changes in the UV/Vis spectral pattern. This apparent contradiction is discussed below.

Proximity between chromophores ($\Delta E \propto |R|^{-3}$) is a necessary but not sufficient condition for a detectable exciton coupling. In fact, some geometries with small distances between the chromophore centers can result in very small, if any, electronic perturbations. The probability of such geometries is not low. For example, none of the arrangements in Figure 3 fulfilling the condition $\cos\theta = 3\cos\phi_1\cos\phi_2$ show any shift in the absorption maximum in respect to the monomer. This is a condition met by more geometries than can be described by the typical magic angle scenario ($\phi_1 = \phi_2 = 52.4°$, when $\theta = 0°$). Nevertheless, in the case of porphyrins, the number of the possible geometries resulting in unshifted absorption bands is small, because of the degeneration of the B-band. This is a consequence of the molecular orbital degeneration in porphyrins, which results in two degenerate or quasi-degenerate transitions with perpendicular polarization (referred as B_x and B_y).[39−41] In metallo and in diprotonated porphyrins with an adequate symmetry pattern of the periphery substituents, the two B transitions are degenerate. For free-base porphyrins, degeneration is theoretically removed but is not detected experimentally. This also occurs in the case of metallo porphyrins without symmetrical substitution patterns (e.g., $ZnDPPS_3$). In the case of dimers and aggregates, the perturbation can only occur between the pairs of transition dipole moments that have the same symmetry ($B_x \leftrightarrow B_x'$, and $B_y \leftrightarrow B'_y$); that is, for fully degenerated oscillators, the linear combination of both orbitals must be taken into account.[42] In this respect, the so-called circular oscillator model has been proposed as a better description of the interaction between porphyrins.[36,43] However, we have only considered the simple point dipole approximation but have taken into account the presence of the B_x and B_y transition dipole moments. We consider that this approximation suffices to infer a qualitative description of the aggregate structure.[36,42] In the simple case of $\theta = 0°$, J and H aggregate scenario, despite the qualitative difference between the x and the y interactions, only one of the two possible transitions is experimentally detected.

Let us consider the dimer geometry of π-stacked porphyrins as the simplest model of the porphyrin aggregates (Figure 4): the centers of the dimer porphyrin rings are shifted about 3.3−3.5 Å and the distance between porphyrin planes is about 4.2 Å (taking into account the dihedral angles of the meso-phenyl substituents). This corresponds to a peculiar geometry giving angles $\phi_1 = \phi_2 \approx 52°$, which in the case of $\theta = 0°$ corresponds to the magic angle scenario ($\Delta E = 0$). However, we propose that the reason for the absence of energy shifts in the B-band of the aggregates of the free bases of symmetrically substituted porphyrins is the breaking of the degeneration through the NH-tautomerism ordering in the aggregate: the monomer shows two degenerate trans NH structures, but for the dimer, two constitutionally different arrangements of the NH tautomerism are possible (Figure 5). Taking into account the saddle ring conformation of the porphyrin ring,[44] in the free-base form, the most stable configuration should be that of "cross" structure (orthogonal pairs of B_x and B_y), where the two opposite pyrrolinic nitrogen atoms of one ring point toward the pyrrolic protons of the other porphyrin, because of favorable polar and hydrogen bonding interactions. This geometry results in a zero

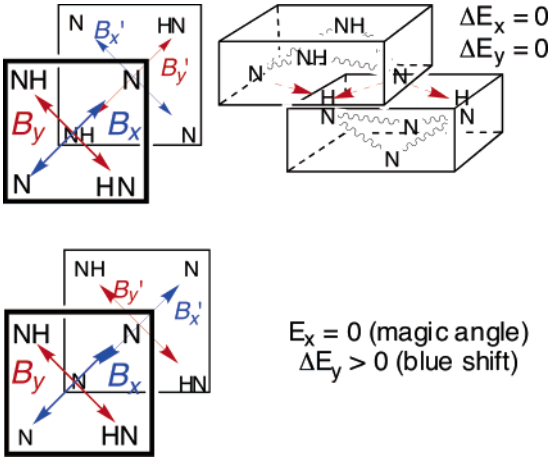

Figure 5. Characteristic free base porphyrin dimer with the two possible arrangements of the NH tautomerism. The orthogonal arrangement is probably the most stable in the case of symmetrically substituted porphyrins (e.g., $TPPS_4$) giving unshifted B-bands (see text). Tautomerism fixation and ordering effects of the periphery substituents (e.g. $DPPS_3$ and $BrDPPS_3$) result in the splitting of the B-band in an unshifted and a blue-shifted absorption.

exciton coupling energy, because $\theta = 0°$ and one of the ϕ angles (see Figures 3 and 5) in the x and in the y perturbation is also equal to 90° (e.g., the case of $TPPS_4$).

Furthermore, the UV/vis spectra of the $DPPS_3$ and $BrDPPS_3$ aggregates, which show a splitting in a blue-shifted and a nonshifted B-band (see Figure 2 and the Supporting Information), can also be explained with the model in Figure 5. It is known that the electronic effect of the sulfonato group at the β-pyrrolic position determines the presence of only one of the two possible trans NH tautomers (22*NH*, 24*NH*).[45] Furthermore, the ^1H NMR results point to a π-stacking structure where the meso-phenyl substituents are overlapped and the sulfonato groups are in the same direction, i.e., the structure on the right of Figure 5, which predicts a spectrum as the experimentally detected one. The structure of these aggregates will be published in more detail elsewhere, but the result to be stressed here, in relation to the influence of aggregation upon the excited states, is that, although some of the tested compounds did not show the H aggregate signature of a blue-shifted absorption, the structure of all tested aggregates correspond to π-stacked arrangements. However, the case of the aggregate of $ZnTPPS_4$ deserves a specific comment. The ^1H NMR spectrum (2 mM) of this compound, despite showing deviations of the Lambert−Beer law at concentrations in the 0.2 mM range, shows the *o*-phenylic protons at lower magnetic fields than the *m*-phenylic ones. This is in contrast to $TPPS_4$ and indicates a small magnetic anisotropy effect of the porphyrin ring. Furthermore, lowering this concentration 1 order of magnitude, or increasing the temperature from 25 to 60 °C (i.e., decreasing aggregation) results in a shift toward low fields of the *o*-phenylic higher than that of *m*-phenylic protons (see the Supporting Information). Nevertheless, it is assumed in a previous work that ZnTPP in organic solvents dimerizes or polymerizes.[38,46] Probably, in addition to a lower tendency to aggregate of $ZnTPPS_4$, in water solution, the aggregate incorporates a water molecule, or molecules, between the Zn atoms, which increases the distance between porphyrins, so that the magnetic effect of the porphyrin ring is lower than in the case of the free-base porphyrins.

Excited Triplet State Decays. The excitation at the B-band ($S_0 \rightarrow S_2$) leads, for all porphyrinoids of Figure 1, to the detection around 450 nm of transient absorptions, with lifetimes in the ms or μs range depending on the absence or presence of O_2 respectively (Figure 6 and the Supporting Information). These long lifetimes point toward excited T_1 states, because the excited S_1 state of porphyrins show lifetimes of the ns−ps order.[27,28] Taking into account the energy differences between these absorptions and their B-bands (≈410 nm) and assuming that the triplet energy should be in the NIR region (<1500 nm), it shows a transition toward an excited state above or around the S_2 energy level.

Let us first present the results obtained in the absence of O_2. Two type of absorption decays were detected: (a) simple monoexponential decays, which could be fitted to $\Delta Abs(t) = C_A \exp[-k_A t]$ kinetics, and (b) biexponential decays that fulfill $\Delta Abs_{total} = C_A \exp[-k_A t] + C_B \exp[-k_B t]$ of a mother-daughter (consecutive) kinetic pathway implying an internal conversion (ic) from the initial triplet (T_{1A}) toward a lower lying triplet state (T_{1B}), i.e., $S_0 \leftarrow T_{1A} \rightarrow T_{1B} \rightarrow S_0$ ($k_{initial\ ISCq} \gg k_A > k_B$). Evidence of a such mother-daughter kinetics was the detection of two absorption maxima ($\Delta\lambda \approx 15$ nm), the initial absorption was of higher energies and the second appeared later and showed a longer lifetime decay than the first (see Figure 7): τ_{1A} was in the ms range and τ_{1B} about 1 order of magnitude larger. The detection in porphyrins of two similar triplet states has recently been described (see Figure 8)[47,48] and attributed to the substitution pattern at the meso positions (i.e., at the bridge C atoms: positions 5, 10, 15, and 20 of the porphyrin ring), which originates a conformational deformation of the porphyrin ring. However, in contrast to the water-soluble porphyrins described here, these previous results were obtained using organic solvent measurements and show two principal differences: (a) lifetimes were 3 orders of magnitude shorter than those described here and (b) our results indicated that most of the tested porphyrinoids show a monoexponential decay for the monomer and a biexponential decay for the aggregate species (see Table 2 and Figure 9). Only the Zn porphyrinates ($ZnTPPS_4$, $ZnDPPS_3$) show the same behavior as monomers and aggregates, monoexponential for $ZnTPPS_4$ and biexponential for $ZnBrDPPS_3$. This behavior agrees with loose character of the Zn porphyrinates

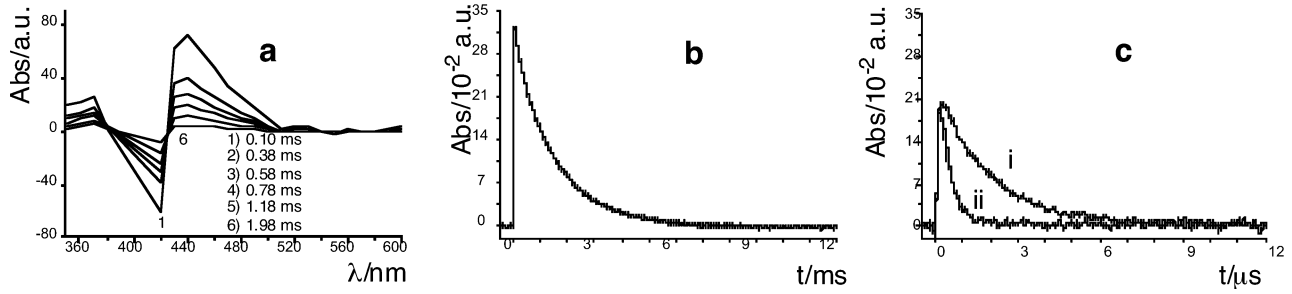

Figure 6. Transitory absorptions of $DPPS_3$ after laser pulse excitation (420 nm). (a) Differential absorption spectrum of a O_2 free 4.0×10^{-5} M in D_2O). (b) Decay of the absorption at 440 nm (1.0×10^{-5} M in D_2O O_2 free). (c) Same conditions as in the previous experiment, but in air (0.24 mM, O_2) and pure O_2 (ii: 1.27 mM O_2) saturated D_2O solutions.

TABLE 2: Triplet Lifetimes at Room Temperature of Monomeric and Aggregates Species in D_2O Solutions[a]

	monomer[b]				aggregate[b]			
	N_2 degassed		O_2 0.24 mM	O_2 1.27 mM	N_2 degassed		O_2 0.24 mM	O_2 1.27 mM
	τ_{1A}/ms	τ_{1B}/ms	τ/μs	τ/μs	τ_{1A}/ms	τ_{1B}/ms	τ/μs	τ/μs
$DPPS_3$	0.74	n.d.	2.4	0.5	0.71	2.12	2.0	0.4
$ZnDPPS_3$	0.15	1.37			0.18	1.90		
$BrDPPS_3$	n.d.	n.d.	n.d.	n.d.	0.03	0.19	1.5	0.4
$ZnBrDPPS_3$	0.14	1.74	2.1	0.6	0.14	1.57	2.2	0.6
$TPPS_4$	2.50	n.d.	2.2	n.d.	0.47	1.63	2.0	n.d.
$ZnTPPS_4$	4.05	n.d.	2.4	0.7	4.17	n.d.	2.7	0.6
MgChl	0.67	n.d.	2.0	n.d.	0.41	2.08	2.2	0.4
$ZnPcS_4$	0.03	n.d.	n.d.	n.d	0.03	0.45	3.0	0.7

[a] τ_A and τ_B correspond respectively to the initial and the second excited states of a mother-daughter kinetics (see text): n.d. = not detected. [b] Corresponding to solutions of concentrations below (monomer) and above (aggregate) the threshold concentration values where aggregation was detected by stationary fluorescence spectroscopy (Table 1).

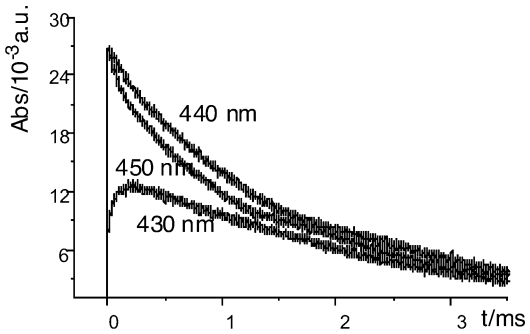

Figure 7. Time evolution, monitored at different wavelengths, of the transitory absorption spectra of $DPPS_3$ ($8.0\ 10^{-6}$ M in D_2O O_2 free) after laser pulsed excitation (λ_{ex} = 420 nm).

in water solution, proposed above because of the presence of water between the Zn atoms, which would imply nonsignificant changes of the porphyrin ring geometry between monomer and aggregates, and as a consequence, similar excited triplet states for monomer and aggregate.

An expected result is the effect of the Br meso-substitution on the quantum yield of the excited states. In this respect, the relative quantum yields of excited triplet state (compare the ordinate values of Figure 9 for $DPPS_3$/$BrDPPS_3$ and $ZnDPPS_3$/$ZnBrDPPS_3$) are smaller for the Br substituted compounds, which must be attribute to the efficient nonradiative deactivation of the excited singlet states toward S_0[49] or, in the case of $BrDPPS_3$ where no excited triplet state could be detected, to very short lifetimes below the detection limit of our experimental equipment.

The results show that the intersystem crossing (ISC) from the excited singlet state manifold occurs only toward T_{1A} but not toward T_{1B}, which points to a strong differentiation of the orbital character of T_{1B} in respect to that of the singlet states. It is worth noting here that, in the cases of monoexponential decay for the monomer and biexponential decay for the dimer, the τ_A lifetimes are very similar or have the same value in the range of the experimental error (Table 2). This suggests that aggregation stabilizes the T_{1B} state below the T_{1A} level. Only in the case of $TPPS_4$ is there a significant decrease of τ_{1A} when we compare monomer (2.5 ms) and aggregate (0.47 ms), the aggregate τ_{1A} value being similar to those of the other porphyrinoids except $ZnTPPS_4$. Monomeric and aggregate $ZnTPPS_4$ also show a τ_{1A} value (4.1 ms − 4.2 ms) 1 order of magnitude larger than the rest of porphyrinoids. In this respect, the common point between these two porphyrinoids is their "symmetrically" meso-tetrakis substitution.

Figure 8 points to the principal conclusions of these results. Aggregation and/or nonsymmetric meso substitution can stabilize T_{1B} below the T_{1A} energy level, so that internal conversion $T_{1A} \rightarrow T_{1B}$ can be detected. This internal conversion is not very fast (see Figure 7) and could be attributed to symmetry constrains between T_{1A} and T_{1B}, which would also explain the absence of ISC from the excited singlet state toward T_{1B}. The stabilization of T_{1B} could be attributed to the conformational deformation of the porphyrin ring, both by the meso-substitution pattern and by aggregation. In fact, the previous detection of a similar triplet state in asymmetrically 5,15 substituted porphyrins, and the increase of ISC, has also been attributed to conformational deformation of the porphyrin ring.[46,47,50,51] This deformation would result in a higher k_A value and aggregation in the stabilization of T_{1B}.

An interesting result concerns the quantum yields of the excited states, as inferred from the C_A and C_B values of the exponential decay fittings, normalized to the sample absorption at the excitation wavelength (Figure 9). Only $ZnPcS_4$ aggregation results in a clear decrease of the T_{1A} and T_{1B} quantum yields. In the case of MgChl, Figure 9 shows an apparent decrease of the initial absorption values when aggregates, but there is the change from monoexponential to biexponential behavior; that is, there is a clear increase in the total initial value $[(C_A + C_B)_{aggr.} > C_{Amonom.}]$ of the monomer. The rest of the porphyrinoids show a clear quantum yield increase by the formation of aggregates. With very high concentrations of aggregates, there are auto-absorption phenomena, but the excited triplet states are always obtained in significant quantum yields. This suggests that the photosensitization ability of the aggregates is not low and in some cases probably higher than those of their monomers.

Figure 9 shows that in the highly diluted range there are two types of behavior. The meso-diaryl substituted porphyrins ($DPPS_3$, $ZnBrDPPS_3$), in very diluted solutions (i.e., before their threshold concentration value for aggregation) show with concentration a decrease of the excited triplet state quantum yield, such as would be expected by the collision between an excited molecule and a nonexcited one. In contrast, the tetrakis-meso substituted $TPPS_4$ and $ZnTPPS_4$ show with concentration an increase of the quantum yield. This, should be attributed to a different mechanism of the aggregate formation: $TPPS_4$ and $ZnTPPS_4$ would show normal aggregation equilibria from monomer to aggregates (monomer and aggregate always present), but the 5,15-diaryl substituted porphyrins would show aggregation after a critical concentration value, such as occurs in the formation of micelles.

In the presence of O_2, excited triplet state decays are all

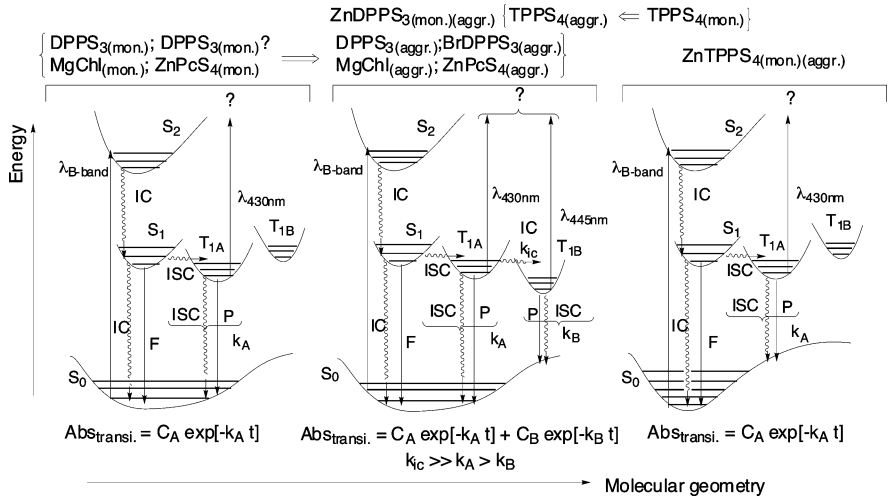

Figure 8. Schematic representation of the photophysical processes following the initial excitation $S_0 \rightarrow S_2$ for the monomers and aggregates.

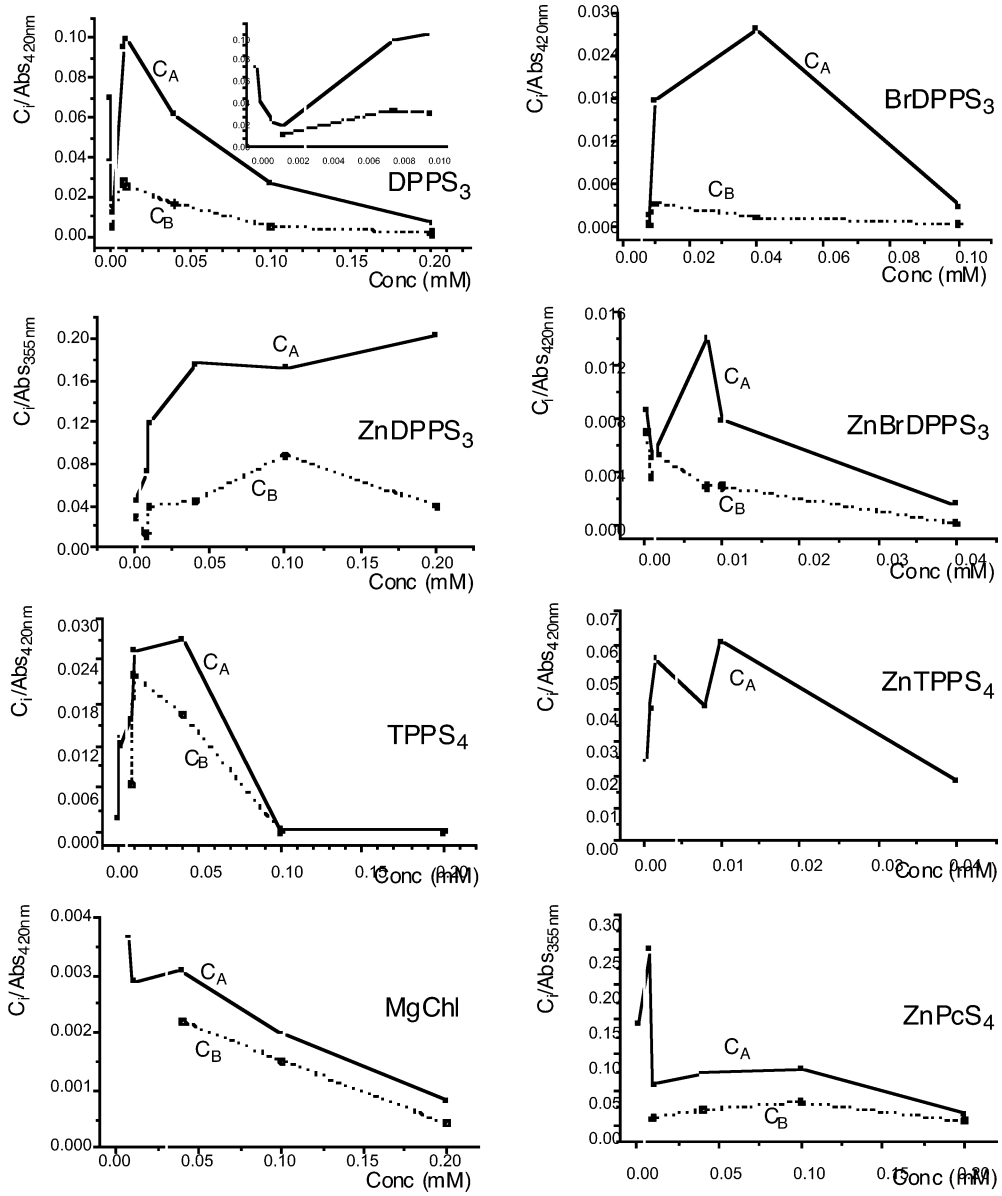

Figure 9. Variation with concentration of the transitory quantum yield, expressed through the transitory absorbance at zero time at the λ_{max} (normalized to the solution absorbance at the excitation wavelength: $\lambda_{ex} = 420$ nm). C_A and C_B are the exponential pre-factors of the decay exponential fittings (see text).

monoexponential, their rates were very similar (≈0.5 μs in pure O_2 saturate solutions: see Table 2) and, in the range of the experimental error, were independent of the porphyrin concentration. Stern−Volmer representations give O_2 quenching

TABLE 3: Quantum Yields (Φ_Δ: See Experimental Section) and Relaxation Rate Constants of $^1O_2$

	Phn	$TPPS_4$	$DPPS_3$	$BrDPPS_3$	$ZnBrDPPS_3$	$ZnTPPS_4$	MgChl	$ZnPcS_4$	$CuPcS_4$
F_D	ref substance	0.43	0.40	0.12	0.15	0.10	0.14	0.09	0.01
k (ms^{-1})	14.8 ± 0.7	17.7 ± 0.5	16.0 ± 0.9	15.4 ± 0.1	20.0 ± 0.7	33.0 ± 0.8	21.0 ± 0.9	24.0 ± 0.9	14.9 ± 0.1
previous Φ_Δ values	0.95[a]	0.66 [b]				0.74[b]		0.01−0.16[c]	0.00[d]

[a] References 24 and 25. [b] Iodine method (S_1 excitation), ref 54. [c] O_2 uptake chemical method, ref 55. [d] Monosulfonate derivative, ref 56.

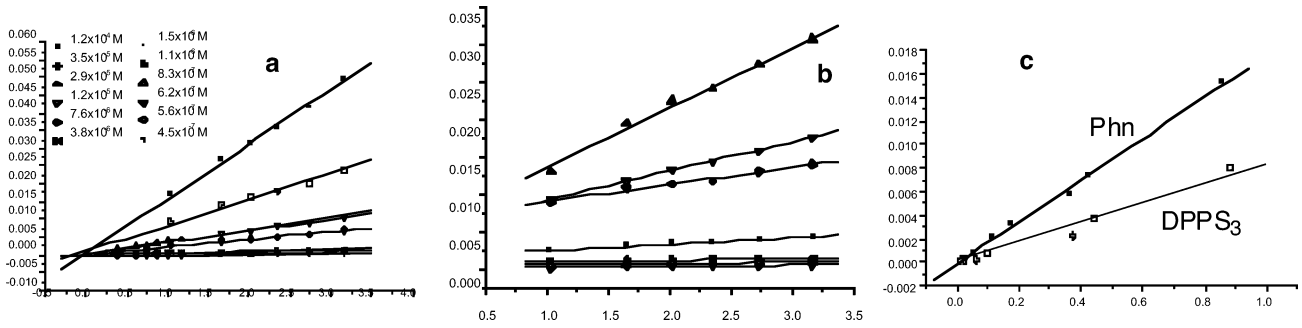

Figure 10. Plots for the calculation of the $^1O_2$ quantum yield of D_2O solutions of $DPPS_3$ (4.5×10^{-7}−1.2×10^{-4} M). Dependence of the $^1O_2$ ($^1\Delta_g$) phosphorescence intensity with the laser energy: (a) Phn (reference substance); (b) $DPPS_3$. (c) Dependence of $\partial S(t=0)/\partial E_l$ with the fraction of absorbed photons ($1-10^{-Abs}$) for Phn ($\Phi_\Delta = 0.97$) and $DPPS_3$ concentration range 1×10^{-7} M to 5×10^{-5} M, i.e., solutions with a significant amount of aggregates: calculated $\Phi_\Delta = 0.47$).

constant values also similar for all compounds (comprised between 1×10^9−2×10^9 mol^{-1} L s^{-1}). These values are similar to those previously reported for these types of porphyrinoids (e.g., 1.8 mol^{-1} L s^{-1} for $TPPS_4$, refs 51 and 52, and 1.9 mol^{-1} L s^{-1} according to our results).

Quantum Yields of $^1O_2$ Photosensitization. $^1O_2$ quantum yields (Φ_Δ) were measured by the $^1O_2(1\Delta_g)$ phosphorescence emission (S) at 1270 nm. The same range of concentrations and experimental conditions as those for the transient state studies were used. Calculations were performed using Phn as reference ($\Phi_\Delta = 0.95$).[25,26] Decay analysis of $S(t)$ was performed in order to determine $S(t=0)$. High concentrations resulting in autoabsorption phenomena were discarded for the $\partial S(0)/\partial E_l$ analysis (see Experimental Section and the Supplementary Information). The presented results correspond to experiments giving linear relationships between the intensity of the $^1O_2$ luminescence signal at time zero [$S(t=0)$] and the laser energy (0.5 mJ $\leq E_l \leq$ 3.25 mJ). The results are summarized in Table 3, in the example in Figure 10 and the Supporting Information.

The phthalocyanines ($ZnPcS_4$, $CuPcS_4$) and the reference compound (Phn) give good straight lines in the plots of the initial phosphorescence intensity [$S(t=0)$] vs the energy of the laser (E_l): extrapolation at zero laser energy affords an approximate zero value for $S(t=0)$ (see the Supporting Information and Figure 10). However, although the rest of compounds gave straight lines, their extrapolation to zero laser energy resulted in values of $S(t=0) > 0$. Furthermore, for several of the porphyrinoids, the crossing values to the $S(0)$ axis build two sets, one for diluted solutions (monomer) and the other one for aggregate solutions, the value being higher in the concentrated solutions. The presence of a constant spurious radiation or of a retarded fluorescence of the samples must be excluded because of the specific experiments performed to detect it and due to the good plots obtained, in the same experimental conditions, for the reference substance and the two phthalocyanines. Despite this, the representations of $\partial S(t=0)$ vs $(1-10^{-Abs})$ show linear plots. However, at very high concentration values most of the porphyrinoids show a positive deviation from linearity (Figure 9), i.e., an apparent increase of the quantum yields with concentration. Below, we discuss the errors that might cause this apparent increase.

The method used for the determination of Φ_Δ is based on the equality, for reference and sample, of the constant terms of eq 1 (Experimental Section). In this respect, the experimental set up ensures that this occurs for V and ν, and it is also a reasonable assumption in the case of k and k_r. Nevertheless, an increase in the refraction index n with the concentration of the sample would result in smaller slope value of $\partial S(0)/\partial E_l$. Such an experimental error is expected to give negative deviations (increase of n with concentration) and not the positive deviations detected. However, at high concentrations, there is a heterogeneous medium of solvent and large aggregates, which could originate light scattering and reflections resulting in an increase in the light path and in consequence an increase of the fraction of absorbed photons. This would lead to an apparently higher quantum yield. More work is in progress to clarify this point. Nevertheless, the significant point to stress here is that the formation of aggregates does not result in the suppression of oxygen photosensitization. The results indicate that for concentrations values corresponding to solutions with a significant amount of π-stacked aggregates the production of $^1O_2$ is of the same order than that of their dilute solutions.

Conclusions

An irregular substitution pattern in the porphyrin periphery and aggregation enables the detection of two excited triplet states. The new excited state is more stable than the current T_1 and is accessible by internal conversion from T_1. In addition to the previous proposed role of the conformational deformation of the porphyrin ring, the results suggest a role of the intermolecular correlation of the NH tautomerism in π-stacked aggregates. The π-stacking in porphyrins (H aggregates), does not suppress the photosensitization quantum yields of $^1O_2$. In fact, for some of the tested porphyrins, H aggregation does not result in a significant decrease of the $^1O_2$ quantum yields. This would explain the efficiency of several porphyrins in photodynamic therapy, despite the expected unavoidable aggregation in cellular sites. It is in this respect that we think that the relationship between photophysical behavior and structure of homo- and heteroassociates of porphyrinoids should be taken into account in the design of photosensitizers for photodynamic therapy.

Acknowledgment. This work was supported by a grant from the Spanish Government (AGL2000-0975). We thank Dr. Josep M. Bofill for valuable discussions and the firm Soquiber-Lab Cosp SA for the gift of chlorophyllin samples.

Supporting Information Available: UV/vis spectra changes with concentration. Study of the aggregation of $TPPS_4$ and $ZnTPPS_4$ by ^1H NMR. Graphics for the calculation of the $^1O_2$ quantum yield. This material is available free of charge via the Internet at http://pubs.acs.org.

References and Notes

(1) Rossbroich, A.; Garcia, N. A.; Braslavsky, S. E. *Chem. Phys. Lett.* **1985**, *148*, 523.

(2) Bonnet, R., McGarvey, D. J.; Harriman, A.; Land, E. J.; Truscott, T. G.; Winfield, U.-J. *Photochem. Photobiol.* **1988**, *48*, 271.

(3) Carmichael, I.; Hug, G. L. In *The Handbook of Organic Photochemistry*; Scaiano, J. C., Ed.; CRC Press: Boca Raton FL, 1989; Vol. 2, p 383.

(4) Tanielian, C.; Wolff, C. *J. Phys. Chem.* **1995**, *99*, 9825.

(5) Andreasson, J.; Zetterqvist, H.; Kajanus, J.; Martensson, J.; Albinsson, B. *J. Phys. Chem. A* **2000**, *104*, 9307.

(6) Shediac, R.; Gray, M. H. B.; Uyeda, H. T.; Johnson, R. C.; Hupp, J. T.; Angiolillo, P. J.; Therien, M. J. *J. Am. Chem. Soc.* **2000**, *122*, 7017.

(7) Andreasson, J.; Kyrychenko, A.; Martensson, J.; Albinsson, B. *Photochem. Photobiol. Sci.* **2002**, *1*, 111.

(8) Bonnet, R. In *Chemical Aspects of Photodynamic Therapy*; Gordon and Breach Sci. Publ.: Amsterdam, 2000.

(9) Sundstrom, V. *Prog. Quantum Elect.* **2000**, *24*, 187.

(10) Sundstrom, V. In *J-Aggregates*; Kobayashi, T., Ed.; World Scientific: Singapore, 1996; p 199.

(11) Witten, W. I. In *The Porphyrins*; Dolphin, D., Ed; Academic Press: New York, 1978; Vol. IIIC, p 303.

(12) Pasternack, R. F.; Collings, P. J. *Science* **1995**, *269*, 935.

(13) Rubires, R.; Crusats, J.; El-Hachemi, Z.; Jaramillo, T.; Lopez. M.; Farrera, A.-A.; Ribo, J. M. *New J. Chem.* **1999**, *23*, 189.

(14) Micali, N.; Monsu' Scolaro, L.; Romeo, A.; Mallamace, F. *Phys. Rev. E* **1998**, *57*, 5766.

(15) Siggel, U.; Binding, U.; Endisch, C.; Komatsu, T.; Tsuchida, E.; Voigt, J.; Fuhrhop, J.-H *Ber. Bunsen-Ges. Phys. Chem.* **1996**, *100*, 2070.

(16) Mosinger, J.; Kliment, V. Jr.; Sejbal, J.; Kubat, P.; Lang, K. *J. Porph. Phthal.* **2002**, *6*, 514.

(17) MacDonald, I. J.; Morgan, J.; Bellnier, D. A.; Paskiewicz, G. M.; Whitaker, J. E.; Lichtfield, D. J.; Dougherthy, Th. J. *Photochem. Photobiol.* **1999**, *70*, 789.

(18) Ellis, R. J. *Curr. Opin. Struct. Biol.* **2001**, *11*, 114−119.

(19) Borsenberger, P. M.; Chowdry, A.; Hoesterey, D. C.; Mey, W. *J. Appl. Phys.* **1978**, *49*, 5555.

(20) Sasaki, F.; Kobayashi, S. *Appl. Phys. Lett.* **1993**, *63*, 2887.

(21) Garcia-Ortega, H.; Ribo, J. M. *J. Porph. Phth.* **2000**, *4*, 564.

(22) Herrmann, O.; Mehdi, S. H.; Corsini, A. *Can. J. Chem.* **1978**, *56*, 1084.

(23) *Landolt-Börstein Zahlenwerte und Funktionen* II Band, Teil 2b; Bartels, J., Borchers, H., Hansen, K., Hellwege, K. H., Schäfer, K. L., Schmidt, E., Eds.; Springer-Verlag: Berlin, 1962; pp 1−20.

(24) Wilkinson, F.; Helman, W. P.; Ross, A. B. *J. Phys. Chem. Ref. Data* **1995**, *24*, 663.

(25) Oliveros, E.; Saurdi-Murasecco, P.; Aminian-Saghafi, T.; Braun, A. M. *Helv. Chim. Acta* **1991**, *74*, 79.

(26) Schmidt, R.; Tanielian, C. Dunsbach, R.; Wolff, C. *J. Photochem. Photobiol. A* **1994**, *79*. 11.

(27) Sessler, J. L.; Gebauer, A.; Vogel, E. In *The Porphyrin Handbook*; Kadish, K. M., Smith, K. M., Guilard, R., Eds.; Academic Press: San Diego, CA, 2000; Vol. 2, pp 1−54.

(28) Khairutdinov, R. F.; Serpone, N. *J. Phys. Chem. B* **1999**, *103*, 761.

(29) Espenson, J. H. In *Chemical Kinetics and Reaction Mechanisms*; McGraw-Hill: New York, 1981; pp 150−152.

(30) Kasha, M.; Rawls, M. A.; El-Bayoumi, M. A. *Pure Appl. Chem.* **1965**, *11*, 371.

(31) Lightner, D. A.; Gawaronski, J. K.; Wijekon, W. M. D. *J. Am. Chem. Soc.* **1987**, *109*, 6354.

(32) Berova, N.; Nakanishi, K. In *Circular Dichroism: Principles and Applications*, 2nd ed.; Berova, N., Nakanishi, K., Woody, R. W., Eds.; Wiley-VCH: New York, 2000; pp 337−382.

(33) Barber, D. C.; Freitag-Beeston, R. A.; Whitten, D. G. *J Phys. Chem.* **1991**, *95*, 4074.

(34) Aratani, N.; Osuka, A. *Org. Lett.* **2001**, *3*, 4213.

(35) Borovkov, V. V.; Lintuluoto, J. M.; Inoue, Y. *J. Am. Chem. Soc.* **2001**, *123*, 2979.

(36) Pescitelli, G.; Gabriel, S.; Wang, Y.; Fleischhauer, J.; Woody, R. W.; Berova, N. *J. Am. Chem. Soc.* **2003**, *125*, 7613.

(37) Abraham, R. A. *J. Magn. Res.* **1981**, *43*, 491.

(38) Hunter, C. A.; Sanders, J. K. M. *J. Am. Chem. Soc.* **1990**, *112*, 5525.

(39) Gouterman, M. *J. Mol. Spectroc.* **1961**, *6*, 138.

(40) Gouterman, M. In *The Porphryins*; Dolphin, D., Ed; Academic Press: New York, 1978; Vol. IIIA, p 1.

(41) Gosh, A. In *The Porphyrin Handbook*; Kadish, K. M., Smith, K. M., Guilard, R., Eds.; Academic Press: San Diego, CA, 2000; Vol. 7, pp 1−38.

(42) Ribo, J. M.; Bofill, J. M:, Crusats, J.; Rubires, R. *Chem. Eur. J.* **2001**, *7*, 2733.

(43) Matile, S.; Berova, N.; Nakanishi, K.; Fleischhauer, J.; Woody, R. W. *J. Am. Chem. Soc.* **1996**, *118*, 5198.

(44) Medforth, C. J.; Senge, M. O.; Smith, K. M.; Sparks, L. D.; Shelnutt, J. A. *J. Am. Chem. Soc.* **1992**, *114*, 9859.

(45) Garcia-Ortega, H.; Crusats, J.; Feliz, M.; Ribo, J. M. *J. Org. Chem.* **2002**, *67*, 2063.

(46) Hunter, C. A.; Leighton, P.; Sanders, J. K. M. *J. Chem. Soc. Perkin Trans. 1* **1989**, 547.

(47) Kyrychenko, A.; Andreasson, J.; Mårtennson, J.; Albinsson, B. *J. Phys. Chem. B* **2002**, *106*, 12613.

(48) Andreasson, J.; Zetterqvist, H.; Kajanus, J.; Mårtennson, J.; Albinsson, B. *J. Phys. Chem. A* **2000**, *104*, 9307.

(49) Borisevich, E. A.; Knyukshto, V. N.; Kozyrev, A. N.; Solovyev, K. N. *Opt. Spektros.* **1993**, *74*, 210.

(50) Kyryhenko, A.; Albinsson, B. *Chem. Phys. Lett.* **2002**, *366*, 291.

(51) Gentemann, S.; Medforth, C. J.; Forsyth, T. P.; Nurco, D. J.; Smith, K.; Fajer, J.; Holten, D. *J. Am. Chem. Soc.* **1994**, *116*, 7363.

(52) Nahor, G. S.; Rabani, J.; Grieser F. *J. Phys. Chem.* **1981**, *85*, 697.

(53) Lee, W. A.; Graetzel, M.; Kalyanasundaram, K. *Chem. Phys. Lett.* **1984**, *107*, 308.

(54) Mosinger, J.; Micka, Z. *J. Photochem. Photobiol. A* **1997**, *107*, 77.

(55) Spikes, J. D.; van Lier, J. E.; Brommer, J. C. *J. Photochem. Photobiol. A* **1995**, *91*, 193.

(56) Rosenthal, I.; Krishna, C. M.; Riesz, P.; Ben-Hur, E. *Radiat. Res.* **1986**, *107*, 136.